Supplementary data

Nuclear dynamics of topoisomerase IIβ reflects its catalytic activity that is regulated by binding of RNA to the C-terminal domain

Table S1. Primer pairs for recombinant construction

Vector	Target	Primer	Sequence (Restriction sites or mutated codons are underlined)	Restriction site
pFlag-CMV-2	1-1614 (full-length)	Sense	5'-GCAGCGGCCGCGCTGCCATGGCCAAGTC-3'	Not I
		Antisense	5'-GTGCTCCCCGGGCACTTAATTAAACATTGC-3'	Sma I
	1-1199 (ΔCTD)	Sense	5'-GCAGCGGCCGCGCTGCCATGGCCAAGTC-3'	Not I
		Antisense	5'-TCCCCCGGGCATCCCTGCCAGAAT-3'	Sma I
	1-1250 (ΔCTD')	Sense	5'-GCAGCGGCCGCGCTGCCATGGCCAAGTC-3'	Not I
		Antisense	5'-TCCCCCGGGCTTCTTCTTCTTCAGCAG-3'	Sma I
	1251-1614 (CTD')	Sense	5'-GAAGCCCGGGGATCCTGATACTACA-3'	Sma I
		Antisense	5'-GTGCTCCCCGGGCACTTAATTAAACATTGC-3'	Sma I
pEGFP-N1	1-1614 (full-length)	Sense	5'-GGCTCGAGCCACCATGGCCAAGTCCAGC-3'	Xho I
		Antisense	5'-GCTCCCGGGGCACTTCATTAAACATTGC-3'	Sma I
	G173I	Sense	5'-GTTACAGGAGGCCGTAATATTTATGGTGCAAAACTT-3'	
		Antisense	5'-AAGTTTTGCACCATAAATATTACGGCCTCCTGTACC-3'	
	L178F	Sense	5'-GGAGGCCGTAATGGTTATGGTGCAAAATTTTGTAATATTTTTAGT-3'	
		Antisense	5'-ACTAAAAATATTACAAAATTTTGCACCATAACCATTACGGCCTCC-3'	
	Y814S	Sense	5'-GATGCTGCAAGCCCCCGTTCTATCTTCACAATGTTAAGC-3'	
		Antisense	5'-GCTTAACATTGTGAAGATAGAACGGGGGCTTGCAGCATC-3'	
pFlag-CMV-2-EGFP	1-1614 (full-length)	Sense	5'-GCAGCGGCCGCGCTGCCATGGCCAAGTC-3'	Not I
		Antisense	5'-GTGCTCCCCGGGCACTAAATTAAACATTGC-3'	Sma I
	1-1199 (ΔCTD)	Sense	5'-GCAGCGGCCGCGCTGCCATGGCCAAGTC-3'	Not I
		Antisense	5'-TCCCCCGGGCATCCCTGCCAGAAT-3'	Sma I
	1201-1614 (CTD)	Sense	5'-TCCCCCGGGAAAGCAGTGAAAGGCAAA-3'	Sma I
		Antisense	5'-GTGCTCCCCGGGCACTAAATTAAACATTGC-3'	Sma I
	1251-1614 (CTD')	Sense	5'-GAAGCCCGGGGATCCTGATACTACA-3'	Sma I
		Antisense	5'-GTGCTCCCCGGGCACTAAATTAAACATTGC-3'	Sma I
	1201-1250 (CRD)	Sense	5'-TCCCCCGGGAAAGCAGTGAAAGGCAAA-3'	Sma I
		Antisense	5'-TCCCCCGGGCTTCTTCTTCTTCAGCAG-3'	Sma I

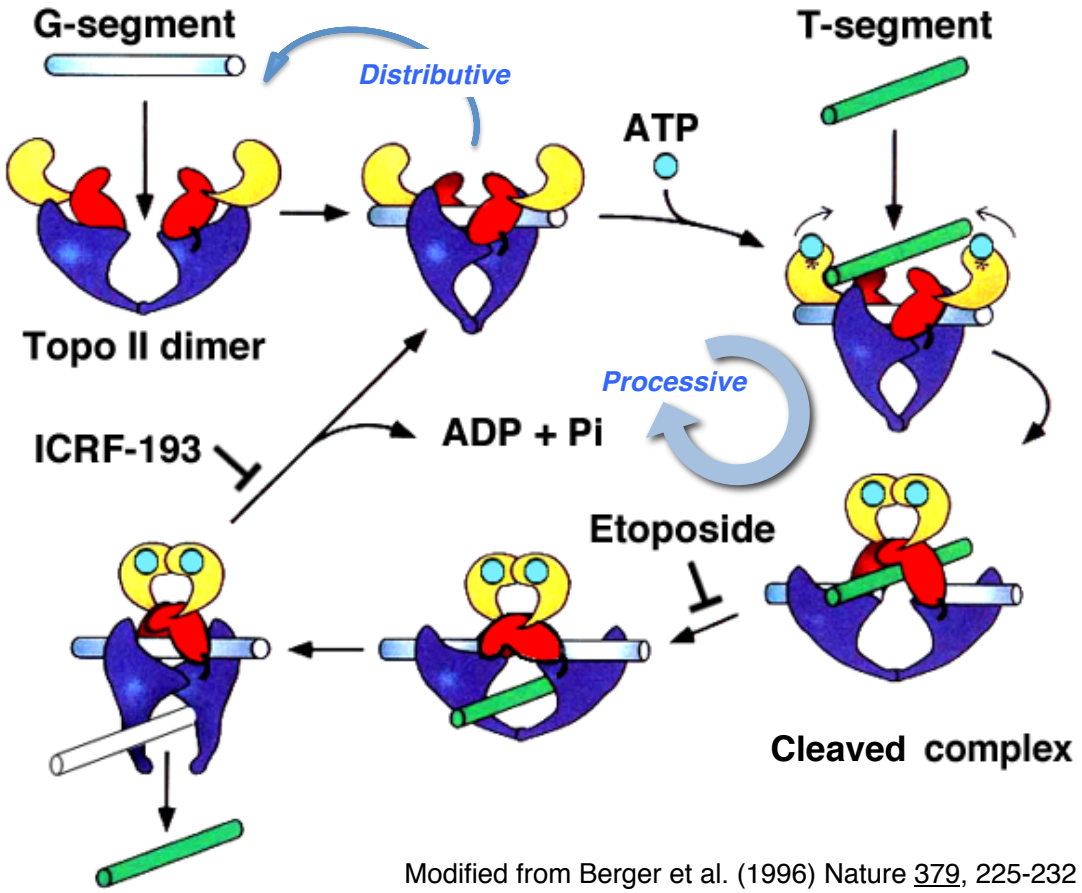

Figure S1. The catalytic cycle of type II DNA topoisomerase.

The duplex DNA entering the topo II dimer (G-segment) is cut and cross-linked transiently to the enzyme in the intermediate called "cleaved complex". After the transfer of another duplex (T-segment) the gap is rapidly re-sealed. The inhibitor etoposide stabilizes the complex to trap the enzyme on DNA ends covalently, whereas ICRF-193 prevents the enzyme from entering the next cycle and clamps the enzyme on G-segment. In the distributive mode G-segment is released at the end of each cycle, while the enzyme enters next cycle without releasing G-segment in the processive mode.

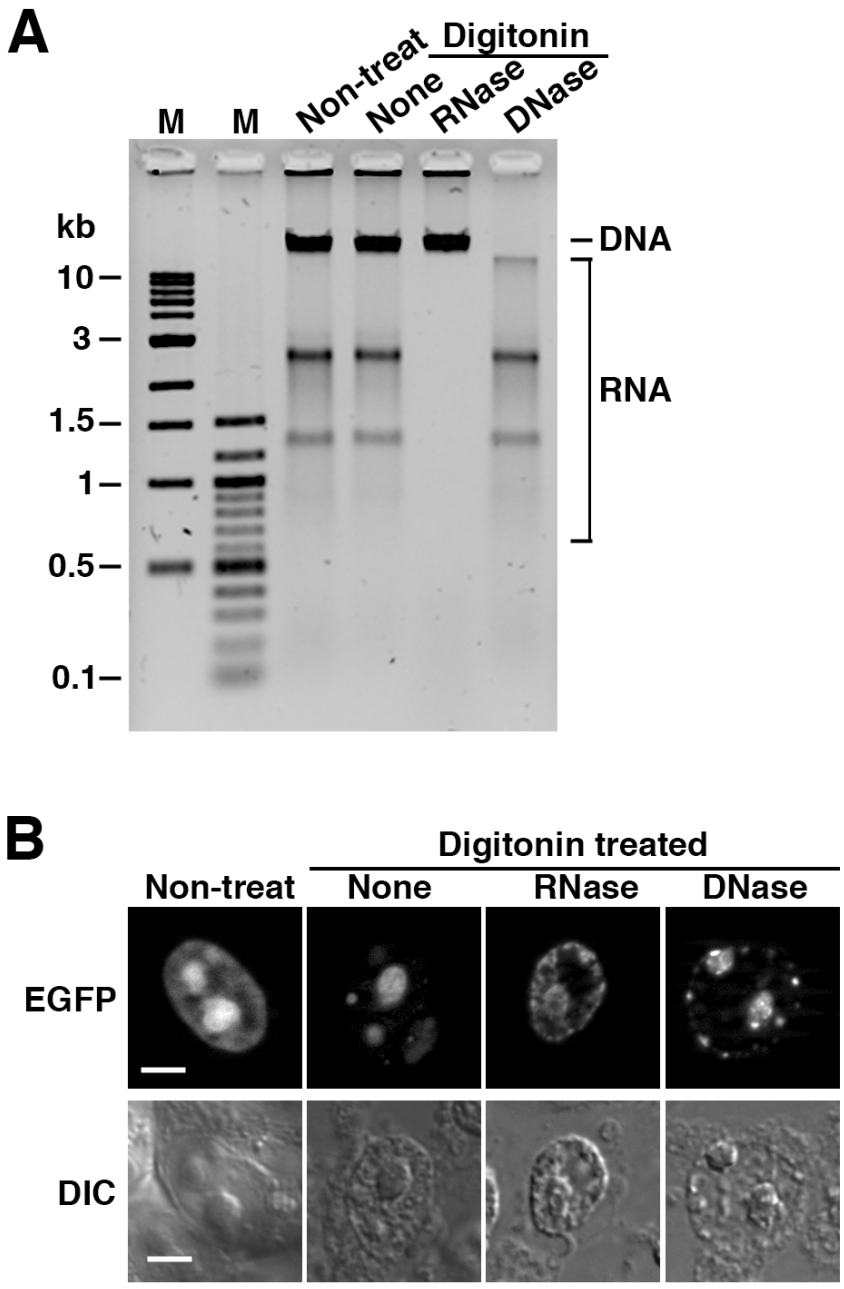

Figure S2. Changes in nuclear localization of topo IIβ by nuclease treatments. **(A)** Selective degradation of RNA/DNA in digitonin-treated cells. Confluent HEK cells were first permeabilized with digitonin and treated with RNase/DNase. After deproteinization with SDS/PK, nucleic acids were separated in 1% agarose gel electrophoresis. **(B)** HEK cells grown on 35-mm glass-bottomed dishes for 48 h were treated with RNase/DNase as in A. EGFP images are shown along with DIC (differential interference contrast) images revealing nucleoli (lower panel). Significant decrease of nucleolar EGFP signal in the central region is evident after RNase treatment. Scale bars, 5 μm.

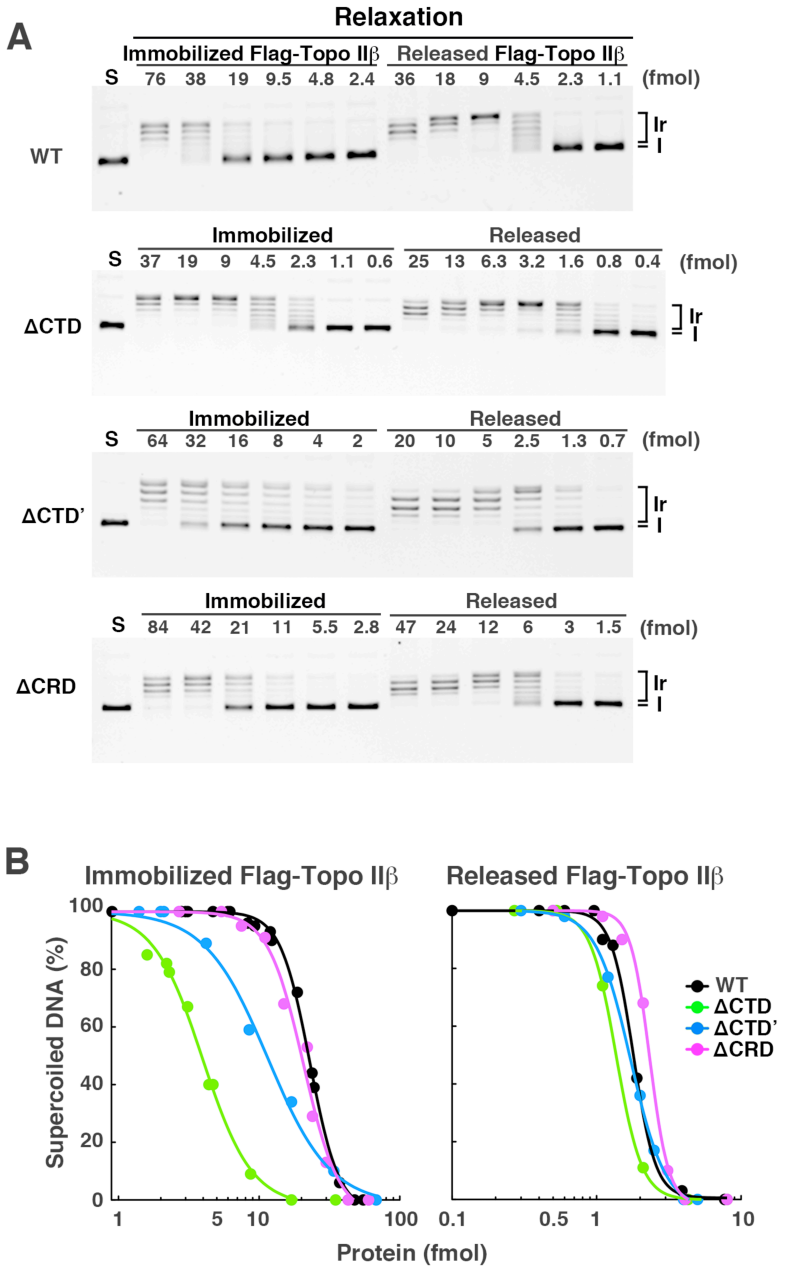

Figure S3. Enzyme dose dependency of relaxation with topo IIβ WT and domain-deletion mutants: bead-bound versus free enzyme. **(A)** Gel images of reaction products. Reactions were set up with decreasing amounts of the enzyme (2-fold dilution series). Amounts of enzyme protein are indicated on the gel top. S, supercoiled substrate. **(B)** Gel bands in A were quantified by densitometry and the percentages of unreacted supercoiled substrate are plotted against enzyme amounts in logarithmic scale. Regression curves were drawn using a software, GraphPad Prism 5 (logistic curve fitting). Note that specific activities among free enzymes are not very different but those for the immobilized mutants with deletions in CTD (ΔCTD and ΔCTD') are significantly higher than others.

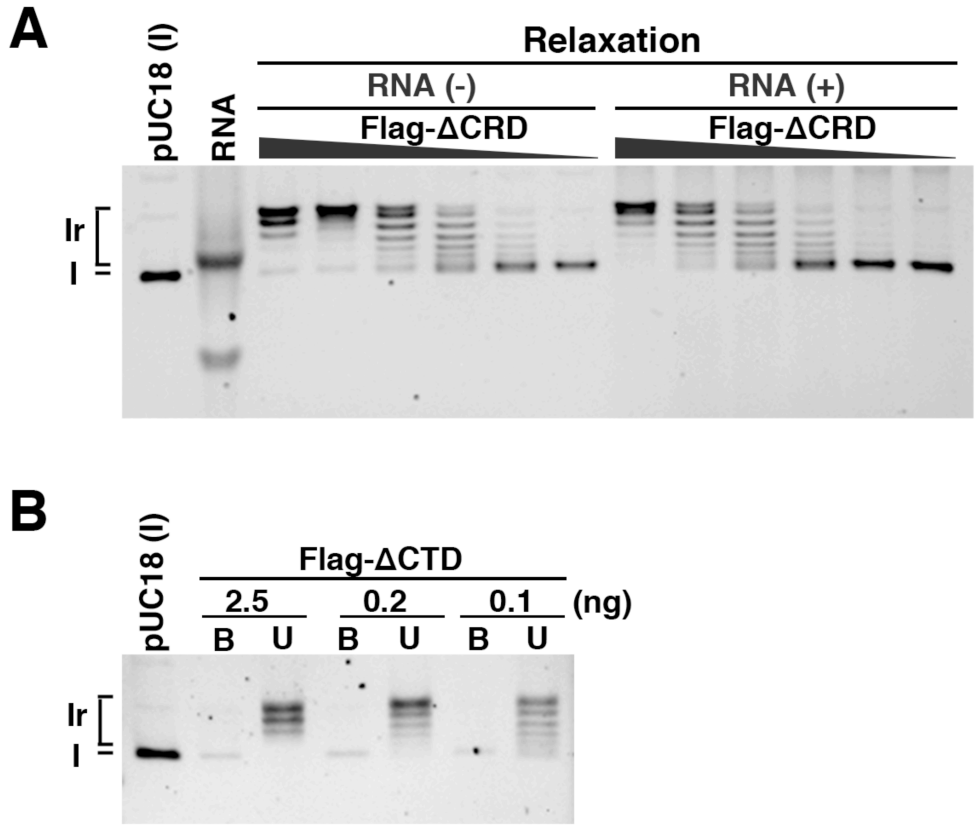

Figure S4. Effects of enzyme dose on RNA inhibition and product retention with topo IIβ CTD mutants. **(A)** Relaxation with decreasing doses of ΔCRD in the absence and presence of RNA. Doses used were 20, 10, 5, 2.5, 1.2, 0.6 fmol of Flag-ΔCRD and 500 ng of total RNA. **(B)** On-bead relaxation assay of ΔCTD. Enzyme-bound (B) and unbound (U) relaxation products were analyzed after the reaction with indicated amounts of Flag-ΔCTD immobilized on magnetic beads.

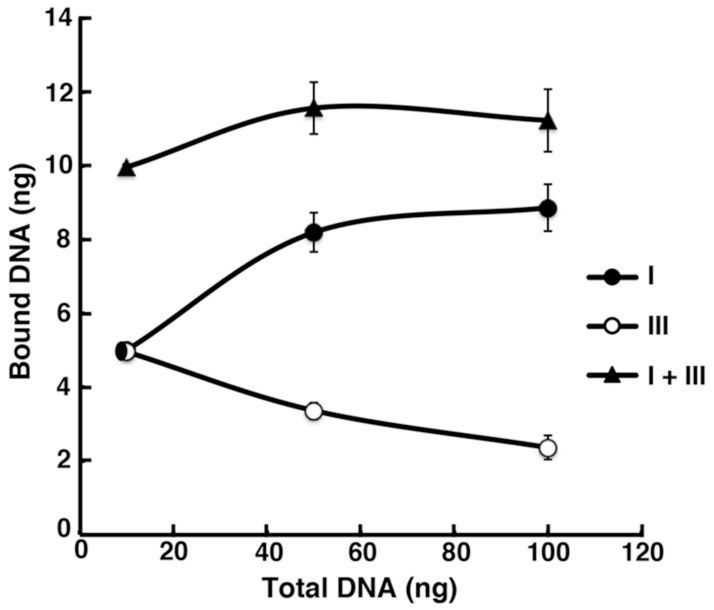

Figure S5. Binding of supercoiled and linear DNA with WT-topo IIβ. Increasing amounts of form I and form III pUC18 DNA (1:1 mixture) were incubated with WT-topo IIβ (80 fmol) immobilized on magnetic beads. DNAs bound on washed beads were separated by agarose gel electrophoresis and quantified by densitometry. Note that total DNA amounts bound on beads (I+III) are almost constant irrespective of added DNA dose.

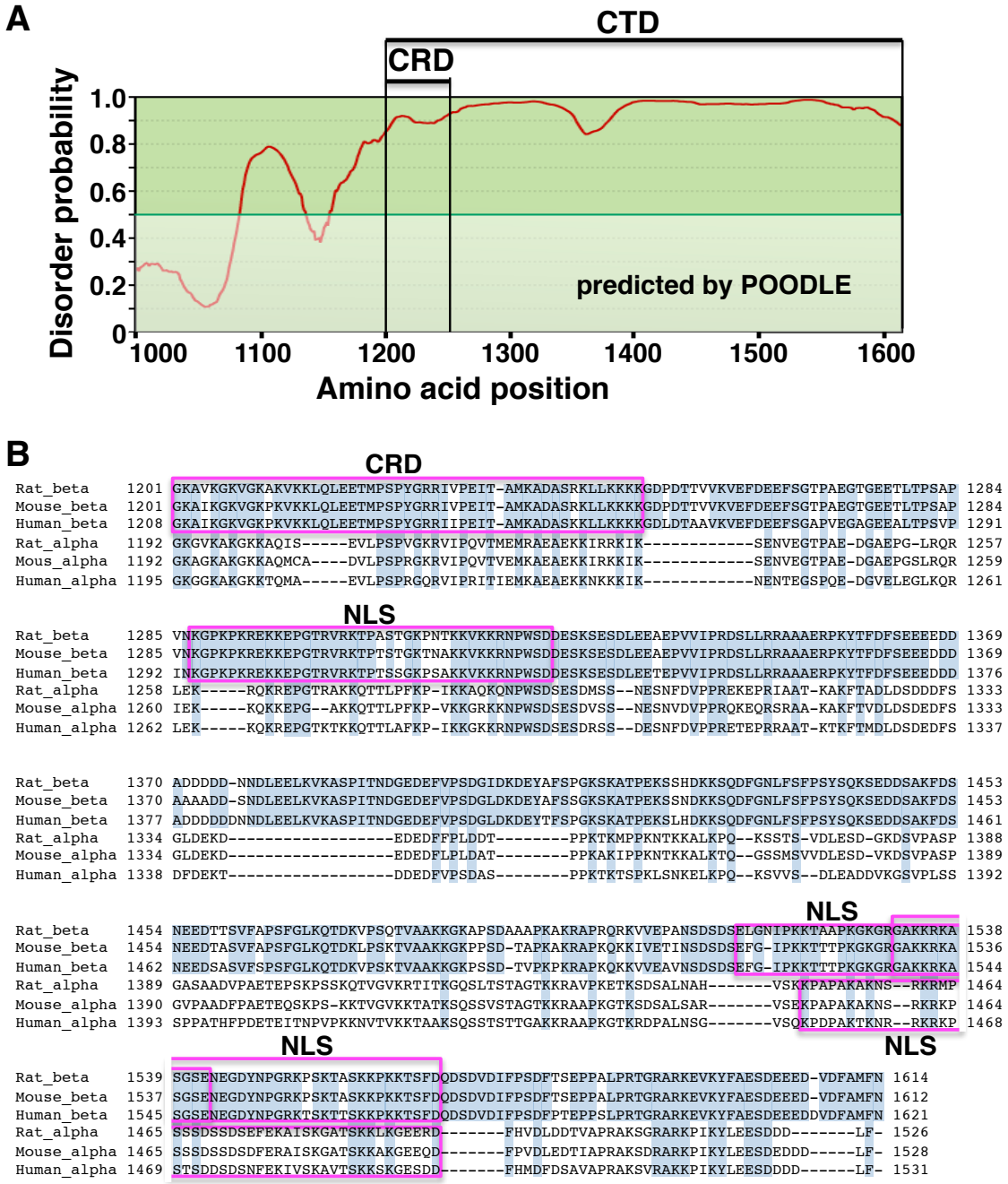

Figure S6. Secondary structure prediction and conserved regions of topo IIβ CTD. **(A)** Rat topo IIβ amino acid sequence 1000-1614 was subjected to the analysis for disordered regions using an online tool called POODLE (mbs.cbrc.jp/poodle/). Positions for CTD and CRD are indicated. The high disorder probability in CTD reflects that the region is poor in distinct secondary structures. **(B)** Amino acid sequence alignment of CTD of topo II isoforms. Sequences aligned are topo IIβ and topo IIα for three species (rat, mouse, human). Numbers on both sides represent residue numbers. CLUSTALX (www.clustal.org/clustal2/) was used as a tool for multiple sequence alignment. Amino acids shared by topo IIβ sequences or by all sequences are shaded.